



Palladium and ceria infiltrated $\text{La}_{0.8}\text{Sr}_{0.2}\text{Co}_{0.5}\text{Fe}_{0.5}\text{O}_{3-\delta}$ cathodes of solid oxide fuel cells

Jing Chen^a, Fengli Liang^a, Bo Chi^a, Jian Pu^a, San Ping Jiang^{b,**}, Li Jian^{a,*}

^a School of Materials Science and Engineering, State Key Laboratory of Material Processing and Die & Mould Technology, Huazhong University of Science and Technology, Wuhan, Hubei 430074, PR China

^b School of Mechanical and Aerospace Engineering, Nanyang Technological University, Singapore 639798, Singapore

ARTICLE INFO

Article history:

Received 22 March 2009

Received in revised form 19 April 2009

Accepted 20 April 2009

Available online 3 May 2009

Keywords:

Solid oxide fuel cells

Palladium

Ceria

Impregnated

Cathode

ABSTRACT

$\text{La}_{0.8}\text{Sr}_{0.2}\text{Co}_{0.5}\text{Fe}_{0.5}\text{O}_{3-\delta}$ (LSCF) cathodes infiltrated with electrocatalytically active Pd and (Gd,Ce) O_2 (GDC) nanoparticles are investigated as high performance cathodes for the O_2 reduction reaction in intermediate temperature solid oxide fuel cells (IT-SOFCs). Incorporation of nano-sized Pd and GDC particles significantly reduces the electrode area specific resistance (ASR) as compared to the pure LSCF cathode; ASR is $0.1 \Omega \text{ cm}^2$ for the reaction on a LSCF cathode infiltrated with 1.2 mg cm^{-2} Pd and $0.06 \Omega \text{ cm}^2$ on a LSCF cathode infiltrated with 1.5 mg cm^{-2} GDC at 750°C , which are all significantly smaller than $0.22 \Omega \text{ cm}^2$ obtained for the reaction on a conventional LSCF cathode. The activation energy of GDC- and Pd-impregnated LSCF cathodes is 157 and 176 kJ mol^{-1} , respectively. The GDC-infiltrated LSCF cathode has a lower activation energy and higher electrocatalytic activity for the O_2 reduction reaction, showing promising potential for applications in IT-SOFCs.

© 2009 Published by Elsevier B.V.

1. Introduction

Perovskite oxides based on lanthanum strontium cobalt ferrite (LSCF) are the most studied mixed ionic and electronic conducting (MIEC) materials for cathode applications in solid oxide fuel cells operated in the intermediate temperature range due to their high mixed ionic and electronic conductivity [1–12]. However, it has been reported that the performance of a LSCF cathode can be enhanced further by dispersing into it a small amount of nano-sized noble metals such as Ag or Pd [13,14]. The overall cell resistance can be decreased by 15.5% at 650°C and 40% at 550°C by impregnating Pd into the LSCF cathode. Adding small amount of Pt into a LSCF cathode is also shown to reduce its electrode polarization resistance [15]. On the other hand, it has been shown that adding another ionic conducting phase such as GDC into a LSCF cathode can improve its performance and the LSCF/GDC composite electrodes show a lower polarization resistance as compared to the pure LSCF cathodes [16–18], indicating that the electrocatalytic activity of a MIEC cathode can be effectively enhanced by introducing into it an ionic conducting phase.

The authors have demonstrated that impregnating or infiltrating nano-size- CeO_2 doped ionic conducting phase and electrocatalytically

active metallic particles such as Pd into (La,Sr) MnO_3 and YSZ cathodes can effectively improve their electrocatalytic activity [19–22]. The impregnation of GDC phase significantly enhances the electrocatalytic activity of the LSM electrodes for the O_2 reduction reactions and simultaneously eliminates the activation effects of the cathodic polarization associated with pure LSM [19]. For example, the LSM electrode impregnated with 5.8 mg cm^{-2} GDC showed a much lower electrode polarization resistance (R_E) than those of LSM/ $\text{Y}_2\text{O}_3\text{-ZrO}_2$ and LSM/GDC composite cathodes and its performance was comparable with those of mixed ionic and electronic conducting oxides (MIEC) such as (La,Sr)(Co,Fe) O_3 and (Gd,Sr) CoO_3 . The performance of LSM cathodes with optimized structure can be improved further with highly dispersed novel metal particles or with doped CeO_2 [19,23,24]. Thus, infiltration or impregnation of ionic conducting oxides such as GDC into a MIEC cathode such as LSCF is expected to increase its electrocatalytic activity by increasing the number of the reactive sites available for the O_2 reduction reaction as observed in the case of LSM. In this study, the electrocatalytic activity of the LSCF cathode infiltrated with Pd and GDC nano-particles via wet impregnation method is measured and the electrode performance for the O_2 reduction reaction is compared with that of LSCF without impregnation treatment.

2. Experimental

Electrolyte substrates were prepared by die pressing 8% mol $\text{Y}_2\text{O}_3\text{-ZrO}_2$ powder (YSZ, Tosoh, Japan), followed by sintering at 1500°C for 4 h in air. The substrate disks were 21 mm in diame-

* Corresponding author. Tel.: +86 27 87557694 fax: +86 27 87557694.

** Corresponding author.

E-mail addresses: mspjiang@ntu.edu.sg (S.P. Jiang), plumarrow@126.com (L. Jian).

ter and 1.2 mm in thickness. $\text{La}_{0.8}\text{Sr}_{0.2}\text{Co}_{0.5}\text{Fe}_{0.5}\text{O}_{3-\delta}$ (LSCF) powder was synthesized by a modified polymer-assisted combustion synthesis method with glucose and acrylamide as fuel and dispersing agent [25]. To prevent the reaction between LSCF electrodes and YSZ electrolyte, a thin GDC interlayer was applied to the YSZ electrolyte disk by firstly screen printing and then sintering at 1250 °C for 2 h in air to form a GDC interlayer protected YSZ electrolyte (GDC/YSZ). The thickness of the GDC interlayer was approximately 8 μm . The LSCF electrode was then screen printed on the GDC/YSZ electrolyte and sintered at 1000 °C for 2 h in air. The thickness of the LSCF cathode was in the range of 8–10 μm and the active electrode area was 0.5 cm^2 .

Impregnation solution of 20 mol.% $\text{Gd}(\text{NO}_3)_3$ + 80 mol.% $\text{Ce}(\text{NO}_3)_3$ ($\text{Gd}_{0.2}\text{Ce}_{0.8}(\text{NO}_3)_x$) was prepared from $\text{Gd}(\text{NO}_3)_3 \cdot 6\text{H}_2\text{O}$ and $\text{Ce}(\text{NO}_3)_3 \cdot 6\text{H}_2\text{O}$ (>99.9%, Aldrich–Sigma). The palladium impregnation solution of 8.5% (w/w) was prepared from $\text{Pd}(\text{NO}_3)_2$ (Alfa Aesar). The Pd- and GDC-infiltrated LSCF composites were prepared by solution impregnation of the $\text{Pd}(\text{NO}_3)_2$ and $\text{Gd}_{0.2}\text{Ce}_{0.8}(\text{NO}_3)_x$ nitrate salts into the porous LSCF layer and the impregnation procedure was repeated four times for each specimen. The infiltrated electrodes were finally fired at 800 °C for 2 h to convert the impregnated $\text{Pd}(\text{NO}_3)_2$ and $\text{Gd}_{0.2}\text{Ce}_{0.8}(\text{NO}_3)_x$ salts to PdO and $\text{Gd}_{0.2}\text{Ce}_{0.8}\text{O}_2$ oxide, respectively [21,22]. The mass of the electrode before and after the impregnation treatment was measured to estimate the loading of impregnated PdO and GDC.

Pt paste was painted on the opposite side of the YSZ electrolyte substrate as the counter and reference electrodes. The counter electrode was positioned symmetrically to the LSCF cathode and the reference electrode was painted in a ring form at the edge of the electrolyte substrate. The gap between the counter and reference electrodes was at least 4 mm, which was 3 times larger than electrolyte thickness. Electrochemical impedance spectra of the electrodes were measured in a frequency range of 0.1 Hz to 100 kHz with signal amplitude of 10 mV at temperatures between 600 and 750 °C using an impedance/gain phase analyzer (Solartron 1260) and an electrochemical interface analyzer (Solartron 1287) at open circuit. The electrode interface (polarization) or area specific resistance (R_E or ASR) was derived from the difference between the low- and high-frequency intercepts at the real impedance axis.

The microstructure of LSCF cathodes and the distribution and formation of impregnated PdO and GDC nanoparticles were analyzed using scanning electron microscopy (SEM) (Sirion 200) and energy dispersive spectroscopy (EDS).

3. Results and discussion

SEM micrographs of fractured cross-sections of LSCF cathodes with and without the PdO and GDC impregnation after the fuel cell testing is shown in Fig. 1. The cathodes were tested at temperatures of 700–800 °C for at least 4–6 h. The original LSCF coating showed a uniform, porous and well sintered structure (Fig. 1a). The LSCF grain size was in the range of 0.2–0.3 μm , and the LSCF grains were well interconnected, forming a rigid and three-dimensional network with sub-micron pores (Fig. 1a). After impregnation with 1.2 mg cm^{-2} PdO, fine particles were uniformly deposited on the surface of LSCF grains and the particle size was in the range of 30–50 nm (Fig. 1b). EDS analysis indicated the presence of the Pd on LSCF electrode after Pd impregnation. In the case of LSCF electrode impregnated with 1.5 mg cm^{-2} GDC, the microstructure is characterized by the formation of fine GDC nanoparticles on the LSCF grains and the size of GDC nanoparticles was in the range of 10–40 nm, which appeared to be smaller than the impregnated PdO nanoparticles (Fig. 1c). The GDC nanoparticles deposited were present in the form of small clusters on LSCF surface, which was also different from the deposited PdO particles which was uniformly distributed on LSCF (Fig. 1b). The overall porosity of LSCF electrode

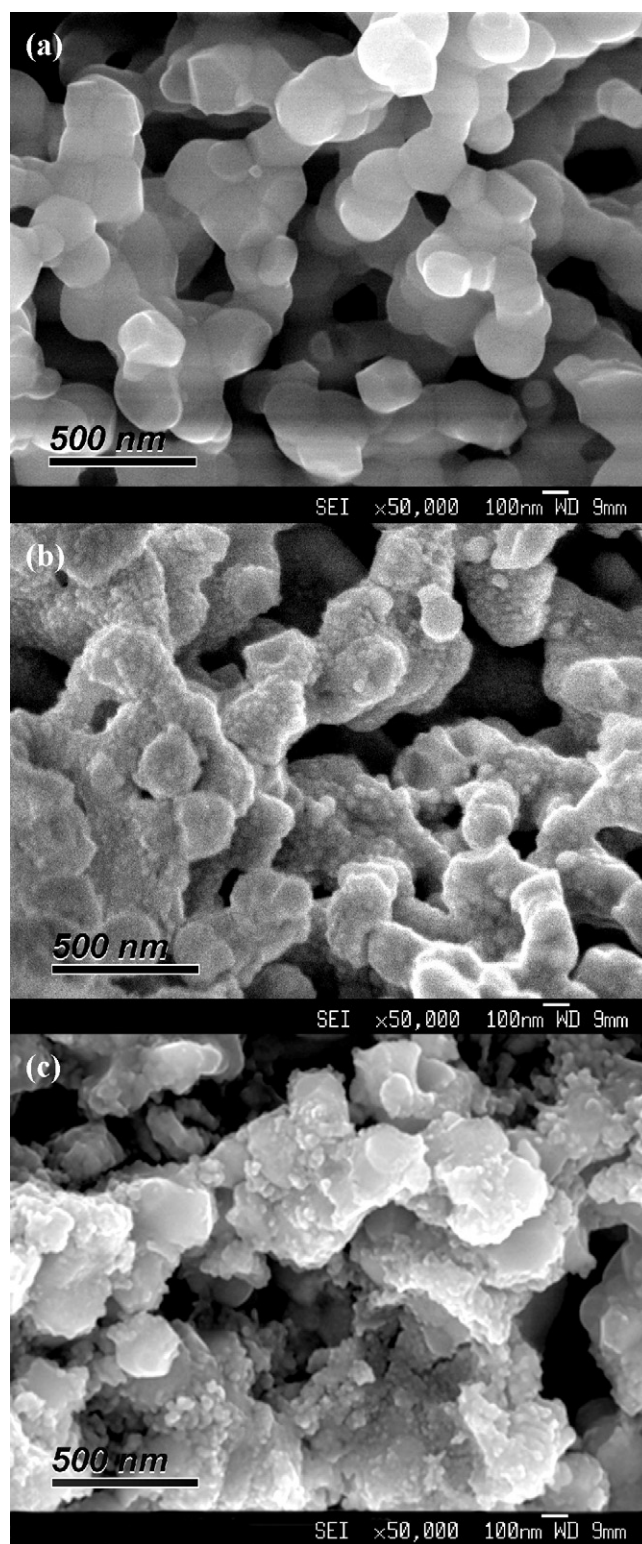


Fig. 1. SEM pictures of fractured cross sections of (a) pure LSCF, (b) PdO-impregnated LSCF, and (c) GDC-impregnated LSCF electrodes after fuel cell testing.

after Pd and GDC impregnation treatment appeared to be similar to that of the LSCF cathode before the impregnation treatment. Despite the test at 600–750 °C for at least 8 h, the agglomeration of impregnated PdO and GDC nanoparticles was not significant.

The electrochemical activity of Pd- and GDC-infiltrated LSCF electrode for the O_2 reduction reaction was investigated by electrochemical impedance spectroscopy and the results are shown

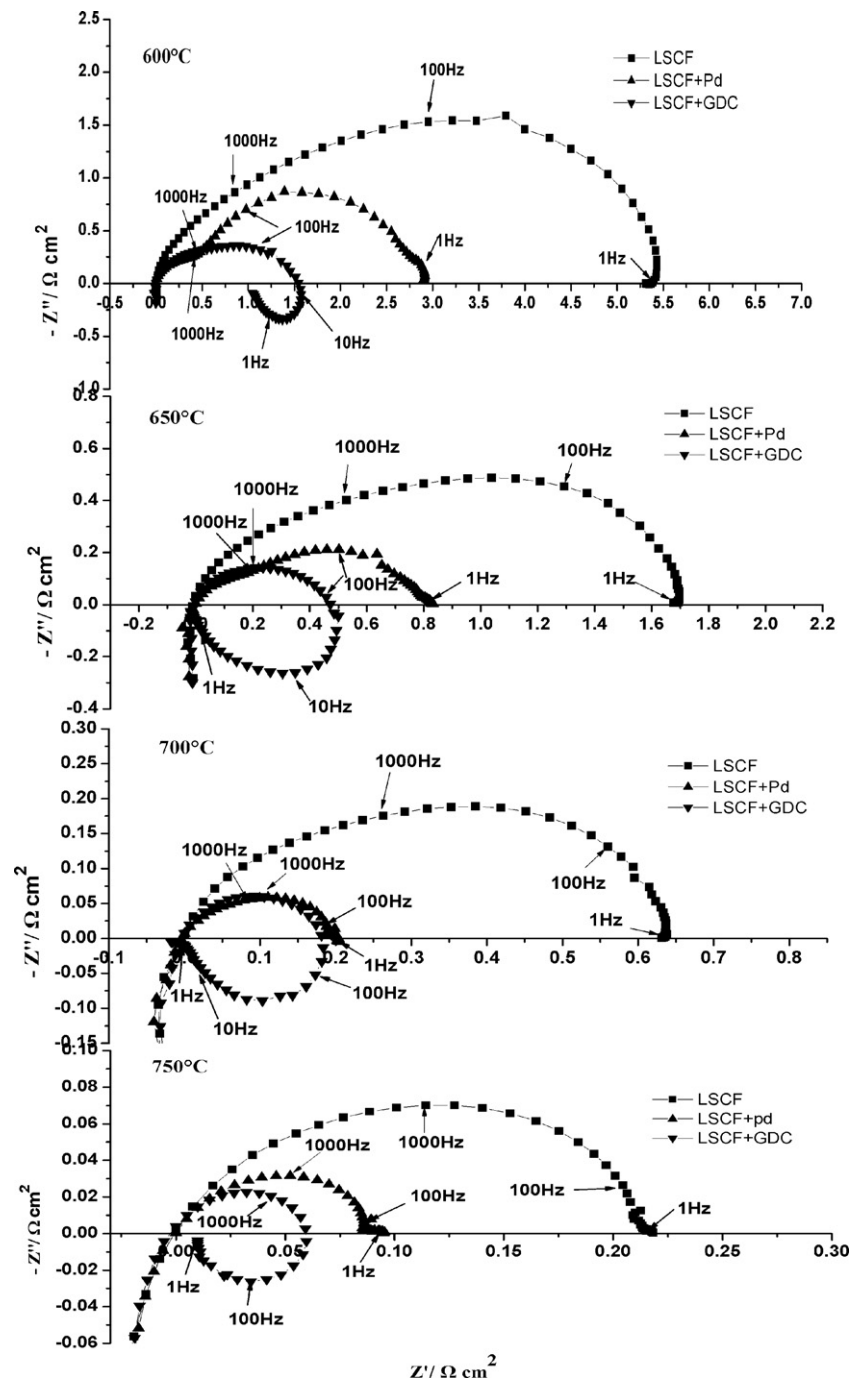


Fig. 2. Impedance curves of the O_2 reduction reaction on (■) pure LSCF, (●) Pd-impregnated LSCF, and (▲) GDC-impregnated LSCF cathodes, measured at 600–750 °C and open circuit in air. The numbers are frequencies.

in Fig. 2. For the O_2 reduction reaction on pure LSCF cathode, the impedance responses were characterized by a large and depressed arc and there was no clear separation between low and high frequency arcs. This is similar to the impedance behavior of LSCF cathodes for the O_2 reduction reaction reported in the literature [3,26]. After Pd and GDC impregnation, there was a significant reduction in the impedance arcs for the O_2 reduction on LSCF electrodes, indicating the enhancement of the electrochemical activity. For the O_2 reduction on the pure LSCF cathode, the overall electrode polarization resistance (R_E) was $0.22 \Omega \text{ cm}^2$ at 750 °C, which was reduced to $0.1 \Omega \text{ cm}^2$ for the reaction on a LSCF cathode impregnated with 1.2 mg cm^{-2} PdO and further to $0.06 \Omega \text{ cm}^2$ on the LSCF cathode impregnated with 1.5 mg cm^{-2} GDC. The ASR for the reac-

tion on GDC-LSCF cathodes of similar microstructure was almost 4 times smaller than that on the pure LSCF under identical testing conditions. At 600 °C, R_E was $5.4 \Omega \text{ cm}^2$ for the reaction on a pure LSCF cathode; it decreased to 2.9 and $1.6 \Omega \text{ cm}^2$ on Pd- and GDC-impregnated LSCF cathodes, respectively. Impregnation of PdO or GDC nanoparticles into LSCF cathode has a significant effect not only on the size of the impedance arcs but also on the characteristics of the impedance responses. There is a significant change in the distribution of low and high frequency arcs for the reaction on the PdO- and GDC-impregnated LSCF cathodes. This shows that the impregnated Pd or GDC phase may have a different effect on the electrode processes associated with low and high frequency arcs for the O_2 reduction reaction.

Esquirol et al. [11] studied the electrode behavior of LSCF for the O_2 reduction reaction and observed two impedance arcs, one at high frequencies at normal partial pressure of oxygen and the other at low frequencies at very low partial pressure of oxygen. This appears to be consistent with the observation that in air, the O_2 reduction reaction on LSCF electrode is characterized by a single impedance arc over the whole frequency range (Fig. 2a). It is noted that the low-frequency impedance decreased significantly with the Pd and GDC impregnation and in the case of GDC-impregnated LSCF, a significant low-frequency loop was developed for the O_2 reduction. The ionic conductivity of GDC is 0.1 S cm^{-1} at 800°C [27], which is higher than the ionic conductivity of LSCF oxides. The higher ionic conductivity of impregnated GDC nanoparticles could be the cause for the significantly reduced electrode resistance for the oxygen migration/diffusion processes associated with

the low frequencies. As reported previously [22], palladium undergoes significant Pd/PdO phase transitions at high temperatures, which depends strongly on temperature, oxygen partial pressure and current. Thus, the possible Pd/PdO transitions occurred under O_2 reduction conditions could be attributed to the reduction in ASR for the reaction by promoting the surface exchange and diffusion process for the oxygen species on LSCF surface [14].

The effect of current treatment on the electrode impedance of O_2 reduction reaction was also studied for pure, Pd- and GDC-impregnated LSCF electrodes. The results are shown in Fig. 3 for the impedance measured at 700°C in air as a function of cathodic current passage at a constant current density of 200 mA cm^{-2} . For the reaction on a pure LSCF, the initial R_E was $0.68 \Omega \text{ cm}^2$ and it reduced slightly with cathodic current passage time (Fig. 3a). This is consistent with previous observation that activation effect of cathodic

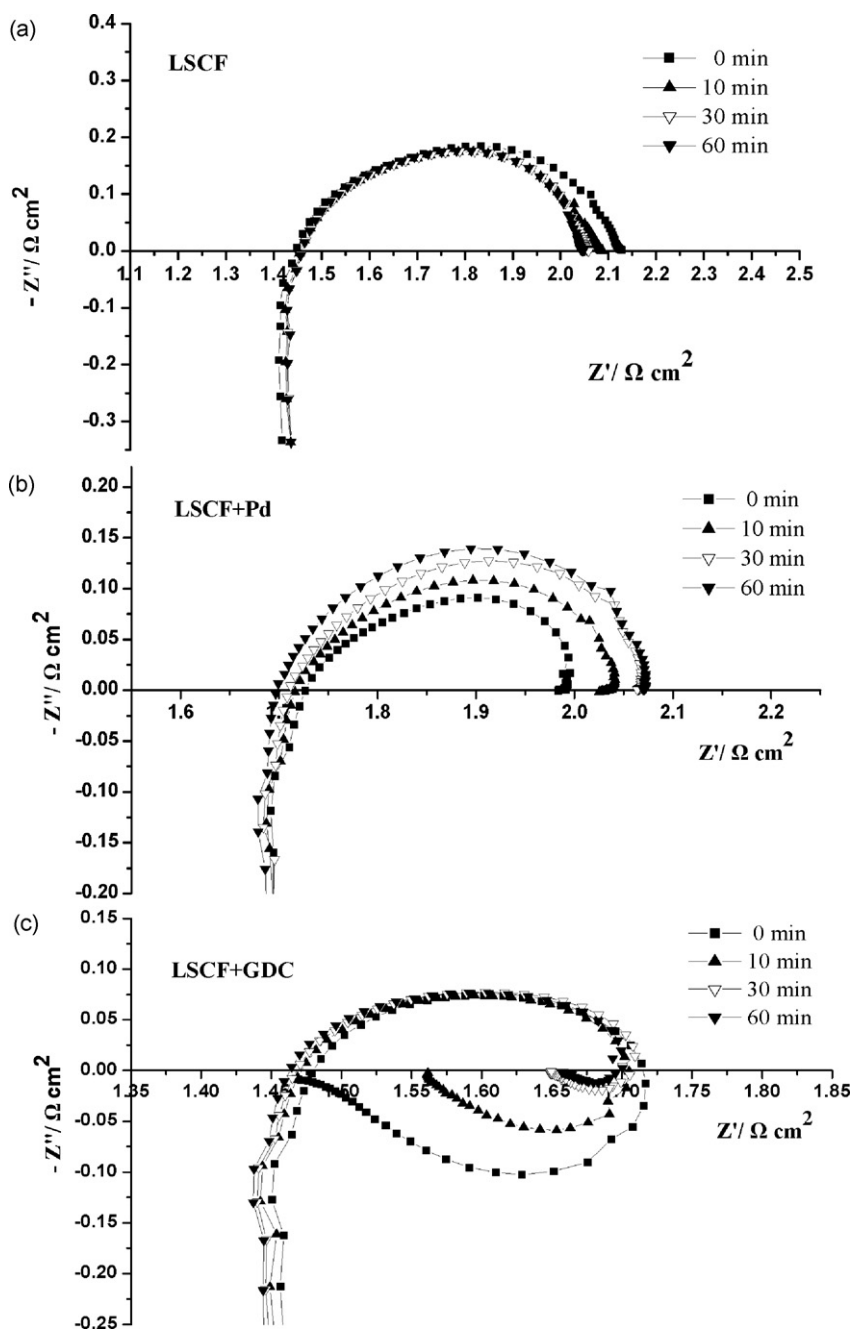


Fig. 3. Impedance curves of the O_2 reduction reaction on (a) pure LSCF, (b) Pd-impregnated LSCF and (c) GDC-impregnated LSCF electrode as a function of cathodic current passage time at 200 mA cm^{-2} at 700°C in air.

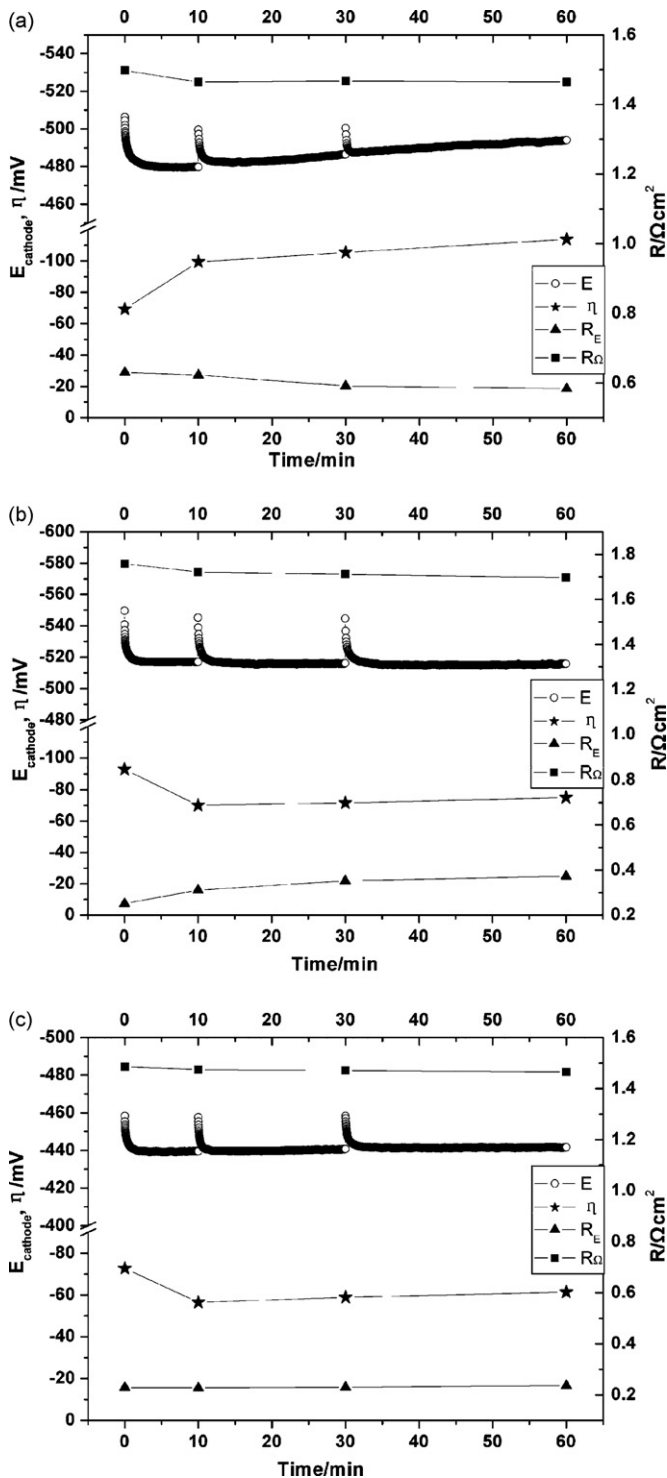


Fig. 4. Polarization curves of the O₂ reduction reaction on (a) pure LSCF, (b) Pd-impregnated LSCF and (c) GDC-impregnated LSCF electrodes as a function of cathodic current passage time at 200 mA cm⁻² and 750 °C in air.

polarization is relatively small for the O₂ reduction on MIEC cathodes such as LSCF [3]. For the reaction on the Pd-impregnated LSCF cathode, the initial R_E was 0.27 $\Omega \text{ cm}^2$, but it increased to 0.37 $\Omega \text{ cm}^2$ after the cathodic current treatment for 60 min. For the reaction on the GDC-impregnated LSCF cathode, the change in R_E was negligible except the reduction in the low-frequency loop (Fig. 3b and c). These results indicate that Pd- and GDC-impregnation has little effect on the initial impedance behavior of the O₂ reduction on LSCF

cathode, but the increase in R_E for the reaction on Pd-impregnated LSCF cathode may be due to the grain growth of the impregnated PdO.

The cathodic polarization potential (E_{cathode}) and overpotential (η) for the O₂ reduction at 750 °C in air on the pure, Pd- and GDC-impregnated LSCF electrodes are plotted against time under a cathodic current passage of 200 mA cm⁻² in Fig. 4. E_{cathode} was measured between LSCF cathode and Pt air reference electrode; the electrode ohmic resistance (R_Ω) and electrode polarization resistance (R_E) were measured by the EIS at open circuit. For the O₂ reduction on LSCF electrode, the change in the cathodic polarization potential with the current passage is much smaller as compared to that on the LSM electrode [3,28]. The polarization losses for the O₂ reduction on the Pd- and GDC-impregnated LSCF electrodes are lower than that on the LSCF electrode. For example, at a current density of 200 mA cm⁻², η was 74 and 61 mV for the reaction on the Pd- and GDC-impregnated LSCF cathode at 700 °C, respectively. Under the same conditions, η was 113 mV on the pure LSCF electrode. Also, the overpotential for the reaction on pure LSCF electrode increases with the current polarization (Fig. 4a), but it decreases with the current polarization for the reaction on Pd- and GDC-impregnated LSCF cathodes (Fig. 4b and c). This shows that the impregnated Pd or GDC phase could also improve the performance stability of the LSCF cathodes.

Fig. 5 compares the temperature dependence of the R_E values of the LSCF-based cathodes measured in the present study with those of the pure LSCF cathodes reported in the literature. For the O₂ reduction reaction on the pure LSCF electrodes, R_E varied greatly

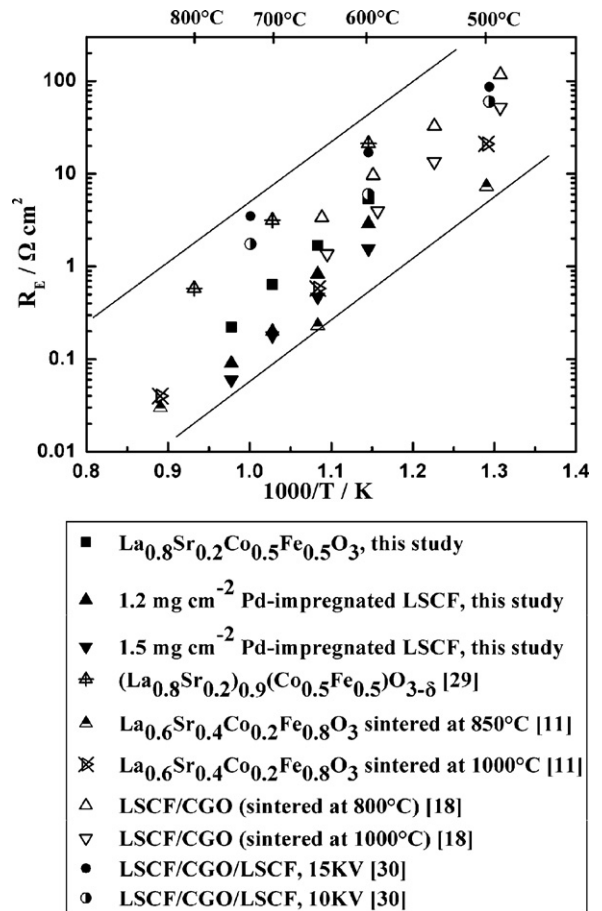


Fig. 5. A comparison of the electrode polarization resistance of Pd-impregnated and GDC-impregnated LSCF electrodes in this study with those of pure LSCF electrodes reported in the literature. Numbers are the references cited and lines are for guides only.

from 0.15 to 3.16 $\Omega \text{ cm}^2$ at 700 °C [11,18,29,30]. With the addition of Pd or GDC phase in the LSCF electrodes, R_E of the composite cathode was reduced to 0.04 $\Omega \text{ cm}^2$ at 700 °C, demonstrating a considerable enhancement in the electrode polarization performance of the GDC-impregnated LSCF cathode over the pure LSCF cathode.

The activation energy was 157, 176, and 159 kJ mol^{-1} for the reaction on pure LSCF, Pd-impregnated LSCF, and GDC-impregnated LSCF cathodes, respectively. Thus, the activation energy for the reaction on the Pd-impregnated LSCF cathode was slightly higher than the value for the reaction on the pure LSCF cathode, but it is similar to the value reported by Sahibzada et al. [14]. However, the activation energy of GDC-impregnated LSCF cathode is comparable to the pure LSCF cathode and it is similar to that reported on the LSCF-GDC composite electrodes where the activation energy remained almost unchanged when the GDC content was less than 35 vol.% [31].

4. Conclusions

LSCF cathodes impregnated with nano-size Pd and GDC particles were successfully fabricated by the wet impregnation/infiltration method. The microstructure of the impregnated LSCF electrodes showed features of uniformly distributed PdO and GDC nanoparticles on the surface of the LSCF grains. The GDC nanoparticles with a size in the range 10–40 nm were present in the form of clusters on the LSCF surface; the size of GDC nanoparticles appeared to be smaller than that of PdO nanoparticles. The nano-structured Pd-LSCF and GDC-LSCF composite cathodes showed significantly lower electrode polarization resistance or ASR than the pure LSCF cathode. For the O_2 reduction on a LSCF cathode impregnated with 1.5 mg cm^{-2} GDC, the overall electrode polarization resistance (R_E) was 0.06 $\Omega \text{ cm}^2$ at 750 °C, which was almost 4 times lower as compared to 0.22 $\Omega \text{ cm}^2$ measured for the reaction on a pure LSCF cathode with a similar microstructure under identical testing conditions. These results indicate the potential promise of Pd- and GDC-impregnation treatment as a method for enhancing the electrocatalytic activities of MIEC cathodes such as LSCF.

Acknowledgements

This research was financially supported by the NSFC project 50571038, 60804031 and the “863” project 2006AA05Z148. SEM

and XRD work was assisted by the Analytical and Testing Center of Huazhong University of Science and Technology.

References

- [1] J.M. Bae, B.C.H. Steele, *Solid State Ionics* 106 (1998) 247.
- [2] B.C.H. Steele, J.M. Bae, *Solid State Ionics* 106 (1998) 255.
- [3] S.P. Jiang, *Solid State Ionics* 146 (2002) 1.
- [4] C.R. Xia, W. Rauch, W. Wellborn, M.L. Liu, *Electrochem. Solid State Lett.* 5 (2002) A217.
- [5] H.J. Hwang, M.B. Ji-Woong, L.A. Seunghun, E.A. Lee, *J. Power Sources* 145 (2005) 243.
- [6] K. Murata, T. Fukui, H. Abe, M. Naito, K. Nogi, *J. Power Sources* 145 (2005) 257.
- [7] V.A.C. Haanappel, J. Mertens, A. Mai, *J. Fuel Cell Sci. Technol.* 3 (2006) 263.
- [8] S.P. Simmer, M.D. Anderson, M.H. Engelhard, J.W. Stevenson, *Electrochem. Solid State Lett.* 9 (2006) A478.
- [9] F. Tietz, V.A.C. Haanappel, A. Mai, J. Mertens, D. Stöver, *J. Power Sources* 156 (2006) 20.
- [10] D. Beckel, A. Dubach, A.N. Grundy, A. Infortuna, L.J. Gauckler, *J. Eur. Ceram. Soc.* 28 (2008) 49.
- [11] A. Esquirol, N.P. Brandon, J.A. Kilner, M. Mogensen, *J. Electrochem. Soc.* 151 (2004) A1847.
- [12] S. Carter, A. Selcuk, R.J. Chater, J. Kajda, J.A. Kilner, B.C.H. Steele, *Solid State Ionics* 53–56 (1992) 597.
- [13] Y. Sakito, A. Hirano, N. Imanishi, Y. Takeda, O. Yamamoto, Y. Liu, *J. Power Sources* 182 (2008) 476.
- [14] M. Sahibzada, S.J. Benson, R.A. Rudkin, J.A. Kilner, *Solid State Ionics* 115 (1998) 285.
- [15] K. Sasaki, J. Tamura, H. Hosoda, T.N. Lan, K. Yasumoto, M. Dokiya, *Solid State Ionics* 148 (2002) 551.
- [16] Y.J. Leng, S.H. Chan, Q.L. Liu, *Int. J. Hydrogen Energy* 33 (2008) 3808.
- [17] F. Qiang, K.N. Sun, N.Q. Zhang, X.D. Zhu, S.R. Le, D.R. Zhou, *J. Power Sources* 168 (2007) 338.
- [18] V. Dusastre, J.A. Kilner, *Solid State Ionics* 126 (1999) 163.
- [19] S.P. Jiang, W. Wang, *Solid State Ionics* 176 (2005) 1351.
- [20] S.P. Jiang, Y.J. Leng, S.H. Chan, K.A. Khor, *Electrochem. Solid-State Lett.* 6 (2003) A67.
- [21] S.P. Jiang, W. Wang, *J. Electrochem. Soc.* 152 (2005) A1398.
- [22] F.L. Liang, J. Chen, J.L. Cheng, S.P. Jiang, T.M. He, J. Pu, J. Li, *Electrochem. Commun.* 10 (2008) 42.
- [23] F. Liang, J. Chen, S.P. Jiang, B. Chi, J. Pu, L. Jian, *Electrochem. Solid-State Lett.* 11 (2008).
- [24] X.Y. Xu, Z.Y. Jiang, X. Fan, C.R. Xia, 15th International Conference on Solid State Ionics, Baden, Germany, 2006, p. 2113.
- [25] L.A. Chick, L.R. Pederson, G.D. Maupin, J.L. Bates, L.E. Thomas, G.J. Exarhos, *Mater. Lett.* 10 (1990) 6.
- [26] J. Liu, A.C. Co, S. Paulson, V.J. Birss, *Solid State Ionics* 177 (2006) 377.
- [27] B.C.H. Steele, A. Heinzl, *Nature* 414 (2001) 345.
- [28] S.P. Jiang, Y.J. Leng, C.H. Chan, K.A. Khor, in: S.C. Singhal, M. Dokiya (Eds.), 8th International Symposium on Solid Oxide Fuel Cells, Paris, France, 2003, p. 422.
- [29] K.K. Hansen, K.V. Hansen, *Solid State Ionics* 178 (2007) 1379.
- [30] C.S. Hsu, B.H. Hwang, *J. Electrochem. Soc.* 153 (2006) A1478.
- [31] H. Zhao, L.H. Huo, L.P. Sun, L.J. Yu, S. Gao, J.G. Zhao, *Mater. Chem. Phys.* 88 (2004) 160.